Journal of Ceramic Processing Research. Vol. 12, No. 1, pp. 70~73 (2011)

J O U R N A L O F
Ceramic Processing Research

Consolidation of a nanostructured Al_2O_3 reinforced Fe-Cr composite by rapid sintering and its mechanical properties

In-Yong Ko[a], In-Jin Shon[a,b,*], Jung-Mann Doh[c], Jin-Kook Yoon[c], Sang-Whan Park[c] and Na-Ra Park[a]

[a]*Division of Advanced Materials Engineering and the Research Center of Advanced Materials Development, Engineering College, Chonbuk National University,Chonbuk, 561-756, Republic of Korea*

[b]*Department of Hydrogen and Fuel Cells Engineering, Specialized Graduate School, Chonbuk National University,Chonbuk, 561-756, Republic of Korea*

[c]*Advanced Fuctional Materials Research Center, Korea Institute of Science and Technology, PO Box 131, Cheongryang, Seoul 130-650, Republic of Korea*

Nano-powders of $Fe_{0.67}Cr_{0.33}$ and Al_2O_3 were synthesized from CrO_3 and 2FeAl powders by high energy ball milling. A highly dense nanocrystalline $3Fe_{0.67}Cr_{0.33}$-Al_2O_3 composite was consolidated by a pulsed current activated sintering (PCAS) method within 2 minutes from mechanically synthesized powders of Al_2O_3 and $Fe_{0.67}Cr_{0.33}$. The average hardness and fracture toughness values obtained were 840 kg/mm^2 and 10 MPa·m$^{1/2}$, respectively.

Key words: Nanosructured materials, Sintering, Mechanical alloying, Mechanical properties, Composite materials.

Introduction

It is increasingly being recognized that new applications for materials require functions and properties that are not achievable with monolithic materials. Metal matrix composites combine metallic properties (ductility and toughness) with ceramic characteristics (high strength and modulus), leading to greater strength in shear and compression and to higher service temperature capabilities. The attractive physical and mechanical properties that can be obtained with metal matrix composites, such as high specific modulus, strength-to weight ratio, fatigue strengh, temperature stability and wear resistance, have been documented extensively [1-5]. Therefore, metal matrix composites are recognized as candidates for aerospace, automotive, bio-materials and defense applications.

Traditionally, discontinuously reinforced metal matrix composites have been produced by several processing routes such as powder metallurgy and various casting techniques. The casting of high-melting metal matrix composites, reinforced with a fine and continuous ceramic phase, is relatively complicated and expensive. New cost-effective (low-temperature, rapid) processing routes need to be developed for the direct fabrication of dense, high-temperature metal matrix composites. The consolidation temperature may be dramatically lowered using a chemical reaction between a low melting metal powder and a ceramic powder. This concept has been utilized in a number of solid replacement reactions [6, 7].

Nanocrystalline materials have received much attention as advanced engineering materials with improved physical and mechanical properties. As nanomaterials possess high strength, high hardness, excellent ductility and toughness, much attention has been paid for their application [8, 9]. The grain size in sintered materials becomes much larger than that in pre-sintered powders due to a fast grain growth during a conventional sintering process. Therefore, controlling grain growth during sintering is one of the keys to the commercial success of nanostructured materials. In this regard, the pulsed current activated sintering method which can make dense materials within 2 minutes, has been shown to be effective in achieving this goal [10, 11].

The purpose of this study was to produce nanopowder using high energy ball milling and dense nanocrystalline Al_2O_3 reinforced Fe-Cr composite within 2 minutes from mechanically alloyed powders using this pulsed current activated sintering method and to evaluate the grain size and its mechanical properties (hardness and fracture toughness).

Experimental Procedure

Powders of 99.99% CrO_3 ((< 5 μm, Junsei chemical co.) and 99% pure FeAl (< 200 μm, Sinagigong, Inc) were used as starting materials. CrO_3 and 2FeAl powder mixtures were first milled in a high-energy ball mill (Pulverisette-5 planetary mill) at 250 rpm and for 10 h. Tungsten carbide balls (8.5 mm in diameter) were used in a sealed cylindrical stainless steel vial under an argon atmosphere. The weight ratio of ball-to-powder was 30 : 1. Milling resulted in a significant reduction of the grain size. The grain sizes of

*Corresponding author:
Tel : +82-63-270-2381
Fax: +82-63-270-2386
E-mail: ijshon@chonbuk.ac.kr

the Fe-Cr alloy and Al_2O_3 were calculated by Suryanarayana and Grant Norton's formula [12];

$$B_r(B_{crystalline} + B_{strain})\cos\theta = k\,\lambda/L + \eta\sin\theta \quad (1)$$

where B_r is the full width at half-maximum (FWHM) of a diffraction peak after instrumental correction; $B_{crystalline}$ and B_{strain} are the FWHM caused by small grain size and internal stress, respectively; k is constant (with a value of 0.9); λ is the wavelength of the X-ray radiation; L and η are the grain size and internal strain, respectively; and θ is the Bragg angle. The parameters B and B_r follow Cauchy's form with the relationship: $B = B_r + B_s$, where B and B_s are the FWHM of the broadened Bragg peaks and the standard sample's Bragg peaks, respectively.

After milling, the mixed powders were placed in a graphite die (outside diameter, 45 mm; inside diameter, 20 mm; height, 40 mm) and then introduced into the pulsed current activated sintering system made by Eltek in South Korea, shown schematically in references [10, 11]. The four major stages in the synthesis are as follows. Stage 1-Evacuation of the system. Stage 2- Application of a uniaxial pressure. Stage 3- Heating of the sample by pulsed current (on time; 20 s, off time; 10 s)of 2800A. Stage 4- Cooling of the sample. The process was carried out under a vacuum of 40 mtorr (5.33 Pa).

The relative densities of the sintered samples measured by the Archimedes method were over 96% of the theoretical value. Microstructural information was obtained from product samples which were polished at room temperature. Compositional and microstructural analyses of the products were made through X-ray diffraction (XRD) and scanning electron microscopy (SEM) with energy dispersive X-ray analysis (EDAX). Vickers hardness was measured by performing indentations at a load of 50 kg and a dwelltime of 15 s on the synthesized samples.

Results and Discussion

X-ray diffraction results of the high energy ball milled powders are shown in Fig. 1(c). The reactant powders of CrO_3 and FeAl were not detected but products, Fe-Cr alloy and Al_2O_3, were detected. From the above result the mechanical alloying occurs completely during the milling. Fig. 2. show a SEM image and X-ray mapping of the mechanically synthesized powder. The milled powders were agglomerated and Fe-Cr alloy and Al_2O_3 were seem to be distributed uniformly from the X-ray mapping. The net reaction can be considered to be a combination of the following two reactions:

$$CrO_3 + 2Al \rightarrow Cr + Al_2O_3 \quad (2)$$

$$Cr + 2Fe \rightarrow 3Fe_{0.67}Cr_{0.33} \quad (3)$$

Reaction Eq.(2) is the well-known, exothermic reaction, for which the standard enthalpy of the reaction ranges from −1,379 to −1,311 kJ over the temperature range of 700 °C (just above the melting temperature of Al, 660 °C)

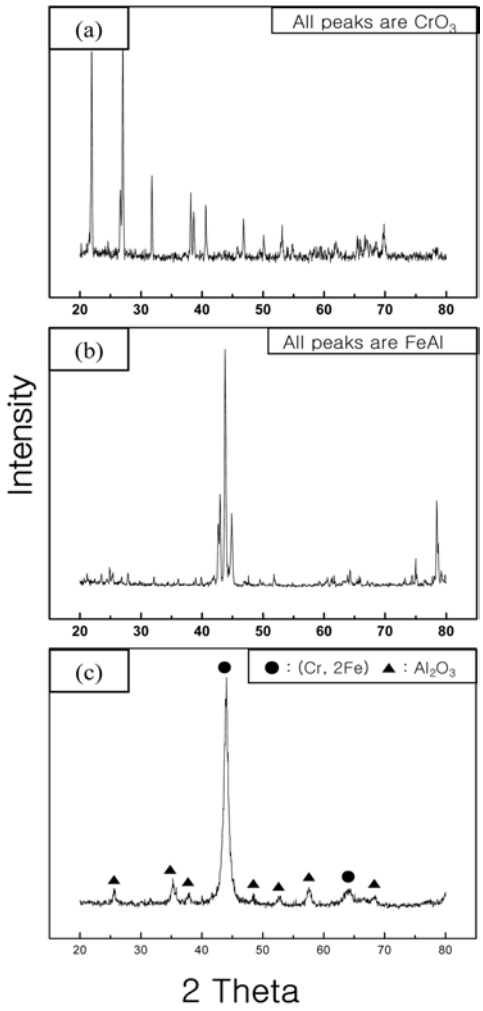

Fig. 1. XRD patterns of raw materials and mechanically alloyed powder: (a) CrO_3, (b) FeAl, and $3Fe_{0.67}Cr_{0.33}$-Al_2O_3.

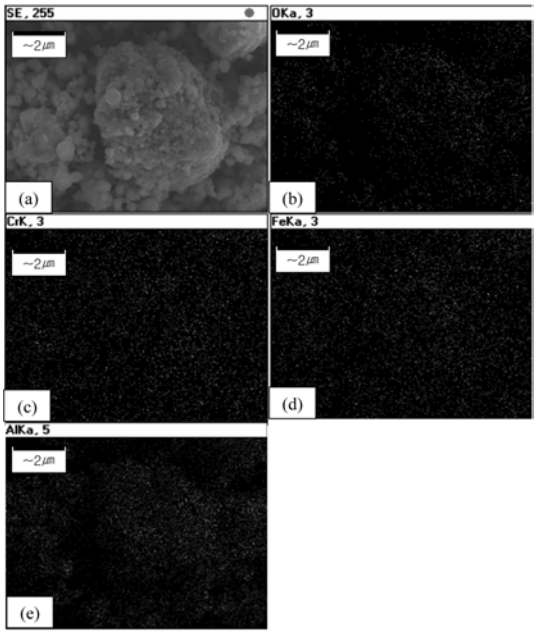

Fig. 2. SEM image and X-ray mapping of $3Fe_{0.67}Cr_{0.33}$-Al_2O_3 powders: (a) SEM image, (b) oxygen mapping, (c) chrominum mapping, (d) iron mapping, (e) aluminum mapping.

to 1800 °C (just below the melting point of Cr, 1863 °C).

The FWHM value obtained from XRD pattern of the milled powder is larger than that of the raw powder due to an internal strain and a reduction of grain size. The average grain sizes of Fe-Cr and Al_2O_3 measured by Suryanarayana and Grant Norton's formula are about 40 nm and 22 nm, respectively.

The variations in shrinkage displacement and temperature with heating time during the processing of the Fe-Cr and Al_2O_3 system are shown Fig. 3. When the pulsed current was applied to the specimen there was a thermal expansion, but this abruptly increased at about 900 °C. An X-ray diffraction pattern of a sample heated to 1210 °C is shown in Fig. 4. Only Fe-Cr alloy and Al_2O_3, were detected in X-ray diffraction pattern. Fig. 5 shows plots of $B_r Cos\theta$ versus $sin\theta$ to calculate the structure parameters, i.e. the average grain sizes of the Fe-Cr alloy and Al_2O_3. The grain size of the Fe-Cr alloy and Al_2O_3 obtained from the X-ray data using Suryanarayana and Grant Norton's formula, were 150 nm and 45 nm, respectively. Fig. 6 shows a

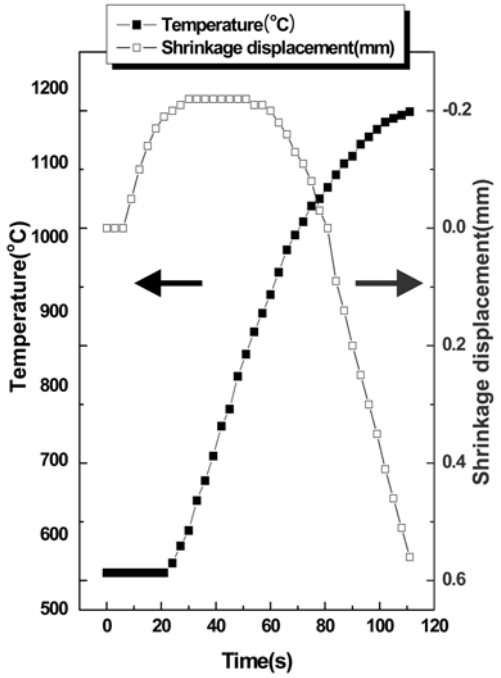

Fig. 3. Variation of temperature and shrinkage displacement with heating time during pulsed current activated sintering of $3Fe_{0.67}Cr_{0.33}$-Al_2O_3 powders.

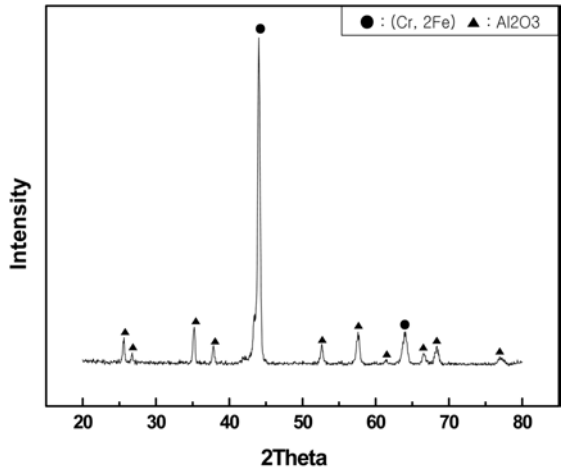

Fig. 4. XRD patterns of the $3Fe_{0.67}Cr_{0.33}$-Al_2O_3 composite heated to 1200 °C.

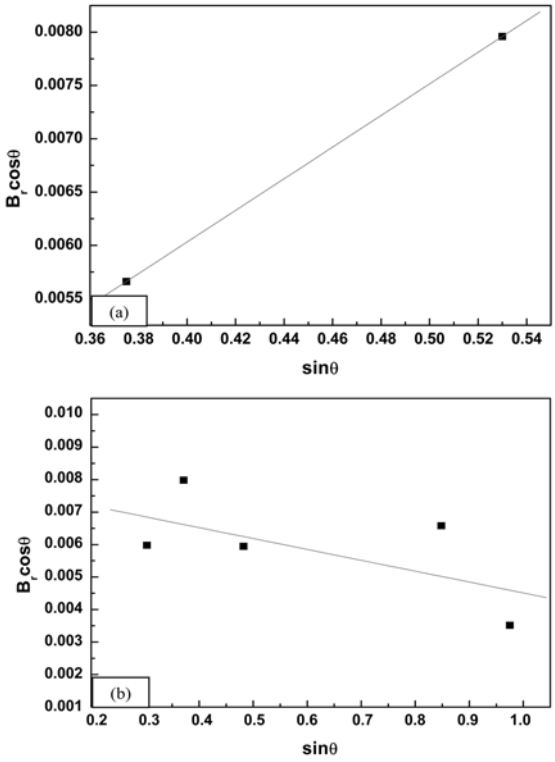

Fig. 5. Plots of $B_r(B_{crystalline} + B_{strain})$ cosθ versus sinθ of $Fe_{0.67}Cr_{0.33}$ and Al_2O_3 in the composite sintered at 1210 °C.

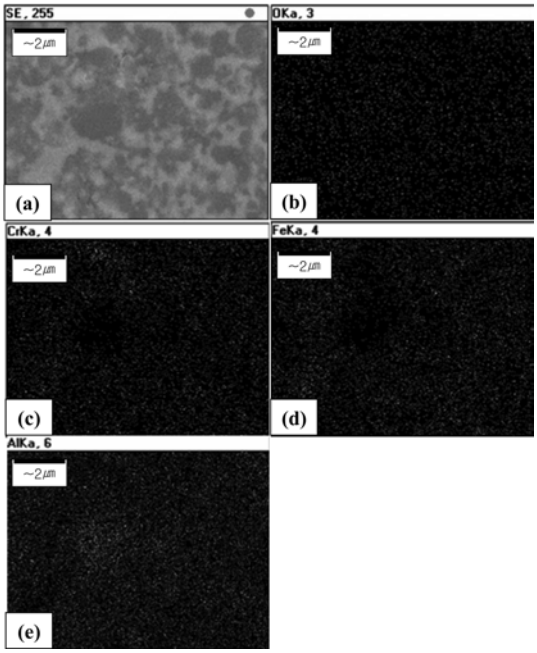

Fig. 6. Scanning electron microscope image and X-ray mapping of $Cr_{0.33}Fe_{0.67}$-Al_2O_3 composite: (a) SEM image, (b) oxygen mapping, (c) chromium mapping, (d) iron mapping (e) aluminum mapping.

scanning electron microscope image and X-ray mapping of the $Cr_{0.33}Fe_{0.67}$-Al_2O_3 composite. The grey phase and the dark phase are Fe-Cr alloy and Al_2O_3, respectively.

Vickers hardness measurements were made on polished sections of the $3Fe_{0.67}Cr_{0.33}$-Al_2O_3 composite using a 50 kg_f load and 15 s dwell time. The calculated hardness value of $3Fe_{0.67}Cr_{0.33}$-Al_2O_3 composite was 840 kg/mm^2. This value represents an average of five measurements. Indentations with large enough loads produced median cracks around the indent. The length of these cracks permits an estimation of the fracture toughness of the material by Niihara *et al.*'s expression [13]:

$$K_{IC} = 0.023(c/a)^{-3/2} \cdot H_v \cdot a^{1/2} \quad (4)$$

where c is the trace length of the crack measured from the center of the indentation, a the half of average length of two indent diagonals, and H_v the hardness.

The calculated fracture toughness value of the $3Fe_{0.67}Cr_{0.33}$-Al_2O_3 composite is about 10 MPa·m$^{1/2}$. As in the case of hardness value, the toughness value is the average of five measurements. The absence of reported values for hardness and toughness on a $3Fe_{0.67}Cr_{0.33}$-Al_2O_3 composite precludes making direct comparison to the results obtained in this study to show the influence of the grain size. However, the hardness and fracture toughness of Al_2O_3 with a grain size of 4.5 μm are reported as 1800 kg/mm^2 and 4 MPa·m$^{1/2}$, respectively [14]. The hardness of the $3Fe_{0.67}Cr_{0.33}$-Al_2O_3 composite is lower than that of monolithic Al_2O_3 but the fracture toughness is higher than the value for Al_2O_3 due to the addition of the ductile Fe-Cr alloy.

Conclusions

Nano-powders of Fe-Cr and Al_2O_3 were made from CrO_3 and FeAl powders by high energy ball milling. Using the pulsed current activated sintering method, the densification of nanostructured $3Fe_{0.67}Cr_{0.33}$-Al_2O_3 composite was accomplished from mechanically alloyed powders. Complete densification can be achieved within a duration of 2 minutes.The relative density of the composite was 96% for an applied pressure of 80 MPa and with the pulsed current. The average grain sizes of Fe-Cr alloy and Al_2O_3 pre- pared by pulsed current activated sintering were about 150 nm and 45 nm, respectively. The average hardness and fracture toughness values obtained were 840 kg/mm^2 and 10 MPa·m$^{1/2}$, respectively.

Acknowledgements

This work was supported by the New & Renewable Energy R&D Program (2009T00100316) of the Ministry of Knowledge Economy, Republic of Korea.

References

1. Jose S. Moya, Sonia Lopez-Esteban, Carlos Pecharroman, Progress in Materials Science 52 (2007) 1017-1090.
2. L. Ceschini, G. Minak and A. Morri, Composites Science and Technology 66 (2006) 333-339.
3. S.C. Tjong, Z.Y. Ma, Materials Science and Engineering 29 (2000) 49-55.
4. DJ. Lloyd, Int Mater Rev 39(1) (1994) 1-6
5. JM. Torralba, F. Velasco, J Mater Process Technol 133(1-2) (2003) 03-206
6. N.R. Park, S.H. Jeon, J.S Park, W. Kim, I.J. Shon, J. Ceramic Processing Research 10 (2009) 774-779.
7. I.Y. Ko, J.H. Park, J.K. Yoon, K.S. Nam, I.J. Shon, Ceramics International 36 (2010) 817-820.
8. MS. El-Eskandarany, J. Alloys & Compounds 305 (2000) 225-238.
9. S Berger, R Porat, R. Rosen, Progress in Materials Science 42 (1997) 311-320.
10. H.C. Kim, I.J. Shon, I.J. Jeong, I.Y. Ko, J.K. Yoon, J. M. Doh, Metals and Materials International 13 (2007) 39-46.
11. H.C. Kim, I.J. Shon, I.K. Jeong, I. Y. Ko, Metals and Materials International 12 (2006) 393-399.
12. C. Suryanarayana, M. Grant Norton, X-ray Diffraction A Practical Approach, Plenum Press, P. 213 (1998).
13. K. Niihara, R. Morena, and D. P. H. Hasselman, J. Mater. Sci. Lett. 1, (1982) 12-16.
14. Mohamed N. Rahaman, Aihua Yao, B. Sonny Bal, Jonathan P. Garino, Michael D. Ries, J. Am. Ceram. Soc. 90 (2007) 1965-1988.